The Identification of Coupled Map Lattice models for Autonomous Cellular Neural Network Patterns

Pan, Y., Billings, S. A. and Zhao, Y.

Department of Automatic Control and Systems Engineering
University of Sheffield
Sheffield, S1 3JD
UK

Research Report No. 949
April 2007

The Identification of Coupled Map Lattice models for Autonomous Cellular Neural Network Patterns

Pan, Y., Billings, S. A. and Zhao, Y.
Department of Automatic Control & Systems Engineering
Sheffield University,
Sheffield, S1 3JD, UK

March, 2007

Abstract

The identification problem for spatiotemporal patterns which are generated by autonomous Cellular Neural Networks (CNN) is investigated in this paper. The application of traditional identification algorithms to these special spatiotemporal systems can produce poor models due to the inherent piecewise nonlinear structure of CNN. To solve this problem, a new type of Coupled Map Lattice model with output constraints and corresponding identification algorithms are proposed in the present study. Numerical examples show that the identified CML models have good prediction capabilities even over the long term and the main dynamics of the original patterns appears to be well represented.

1 Introduction

Spatiotemporal pattern formation is common in many disciplines of science and engineering including chemistry, physics and biology. For example, periodic, chaotic, oscillatory and Turing patterns have been observed in concentrations of chemically reacting and diffusing systems [17] [21] [10]. The reaction-diffusion dynamics of spatial pattern formation have also been used to model the development of patterns in fish, seashells and animal coats [3] [19] [20]. Similar structures such as travelling waves and Turing patterns

have been observed in biological systems [18]. As a consequence of the common occurrence of spatial patterns, the discovery of new pattern formation phenomenon is potentially of great research interest. Several authors have therefore studied the analysis and simulation of a variety of spatiotemporal models which produce various interesting spatial patterns. The Partial Differential Equation (PDE) models where the variables evolve continuously over the continuous space and time domain have been used to describe a wide class of spatiotemporal behaviours, including the Gray-Scott model [11], Fitz-Hugh-Nagumo model and Belousov-Zhabotinsky model.

Cellular Neural Networks (CNN) [7] which are defined by the coupling of cells continuously evolving over a discrete spatial lattice have also been widely applied to model complex spatiotemporal patterns. Because of the simplicity and easy implementation in hardware, CNN's have found numerous applications in image and video signal processing, and in pattern recognition. Apart from providing an alternative paradigm for simulating nonlinear Partial differential Equations, CNN models have been shown to generate propagating waves, patches, checkerboard patterns, stripes and reaction-diffusion type patterns [2] [23] [13]. Further research on the emergence and complexity of spatiotemporal systems has revealed that CNN can give rise to many interesting patterns by tuning the parameters in the CNN templates. Hence, the problem of deriving the corresponding CNN templates for specific spatiotemporal behaviours has also been recently investigated [13].

The Coupled Map Lattice model which was initially introduced in the 1980s by Kaneko [14][15] has been widely used to model spatiotemporal systems. The CML model is discrete in time and space and has a continuous state value. A CML is a d-dimension lattice where each site evolves in time through a discrete map which describes the influence of the past state and neighboring sites. It has been shown that CML models can exhibit complex spatiotemporal behaviors, including chaos, intermittency, travelling waves and Turing patterns [16]. Compared with PDE models, CML models are computationally more efficient and have been used to study spatiotemporal systems in a wide class of scientific subjects.

Given the various patterns produced by CNN models, the inverse problem of how to model these spatiotemporal behaviours from observed data will be considered in this paper. As a subset of CNN patterns, the identification problem of autonomous CNN patterns using CML models is the main focus of the present study. Due to the special nonlinear structure of CNN, it is not easy to obtain CML models for these patterns using general identification algorithms. In the present study, an identification algorithm based on a CML model is introduced based on an amended Orthogonal Forward Regression (OFR) algorithms for these special classes of spatiotemporal behaviours. The

coefficients of the identified model are adjusted by using an amended error sequence from the model prediction to enhance the prediction performance of the final model.

The paper is arranged as follows. Section 2 gives a general description of autonomous Cellular Neural Networks and Coupled Map Lattice models for spatiotemporal systems. Section 3 introduces a correlation based method to select the sampling interval for the identification data. Then, the new identification method which is based on a modified OFR algorithm is proposed. Some numerical examples of CNN patterns are included in Section 4 to illustrate the application of the new identification methods and to demonstrate the performance of the identified CML models to identify these systems.

2 Autonomous Cellular Neural Networks and Coupled Map Lattice Models

2.1 Coupled Map Lattice models

Consider the input-output CML model for time and spatially invariant spatiotemporal systems[8] [9]

$$y_i(k) = f(q^{n_y} y_i(k), q^{n_u} u_i(k), q^{n_y} s^{m_y} y_i(k), q^{n_u} s^{m_u} u_i(k)) + \varepsilon_i(k) \tag{1}$$

where $i \in I^d$ is the spatial index of a d-dimensional space and $k = 1, 2, \ldots,$ is the temporal index; $y_i(k)$, $u_i(k)$ and $\varepsilon_i(k)$ are the output, input, model residual sequences respectively, and $q^n(k)$ is a temporal backward shift operator

$$q^n = (q^{-1}, q^{-2}, ..., q^{-n}) \tag{2}$$

so that

$$\begin{aligned} q^{n_y} y_i(k) &= (y_i(k-1), y_i(k-2), ..., y_i(k-n_y)) \\ q^{n_u} u_i(k) &= (u_i(k-1), u_i(k-2), ..., u_i(k-n_u)) \end{aligned} \tag{3}$$

In (1), s^m is a multi valued spatial shift operator

$$s^m = (s^{p^1}, s^{p^2}, ..., s^{p^m}) \tag{4}$$

where $p^j \in I^d$ is the spatial translation multi index, such that

$$\begin{aligned} s^{m_y} y_i &= (y_{i-p^1}, y_{i-p^2}, ..., y_{i-p^{m_y}}) \\ s^{m_u} u_i &= (u_{i-p^1}, u_{i-p^2}, ..., u_{i-p^{m_u}}) \end{aligned} \tag{5}$$

The parameters m_y, m_u denote the maximum spatial radius associated with the output y and input u.

2.2 Autonomous Cellular Neural Networks

A CNN is said to be autonomous if the cells do not have external inputs. The standard form of an autonomous CNN defined over a two dimensional $N \times N$ array can be expressed by the following equation,

$$\dot{x}_{i,j} = -x_{i,j} + z_{i,j} + \sum_{n,l \in S_{i,j}} a_{n,l} y_{n,l} \tag{6a}$$

$$y_{i,j} = g(x_{i,j}) \tag{6b}$$

where $(i, j) \in N \times N$ denotes the spatial site and $x_{i,j}$, $y_{i,j}$ are state space variables and output variables respectively. The output function $g(\cdot)$ here is defined as the three segment piecewise linear saturation function.

$$g(x_{i,j}) = \frac{1}{2}(|x_{i,j} + 1| - |x_{i,j} - 1|) \tag{7}$$

The CNN dynamics are usually restricted to be inside the boundary of the array $N \times N$. Consequently, additional boundary conditions need to be specified for model (6). Three kinds of boundary conditions are most commonly used, Dirichlet (fixed), Neumann (zero flux) and Toroidal (periodic) boundary conditions. With specific boundary conditions, the dynamics of the standard CNN (6) is then only determined by the CNN template which is composed of the threshold $z_{i,j}$ and the neighbourhood coupling matrix $A = \{a_{n,l}\}$. If the neighbourhood radius of every cell is set to be $r = 1$, the feedback template A of a two dimensional CNN can be described as follows.

$$A = \begin{pmatrix} a_{-1,-1} & a_{-1,0} & a_{-1,1} \\ a_{0,-1} & a_{0,0} & a_{0,1} \\ a_{1,-1} & a_{1,0} & a_{1,1} \end{pmatrix} \tag{8}$$

The behaviours of different pattern formations of standard autonomous CNN models have been extensively studied with various A-templates using state space stability theory. Perturbing the unstable equilibrium state with small and random disturbances, the symmetry of the unstable equilibrium is broken and complex patterns will be formed. As can be seen from the piecewise function $g(\cdot)$, the output trajectories of all cells can be divided into three regions: a linear region and two saturation regions. Because the output function $g(\cdot)$ is continuous and bounded, all trajectories defined by the standard CNN model (6) will converge to an equilibrium state when certain conditions are satisfied [7].

The identification task considered in this paper is to determine the unknown discrete CML model $f(\cdot)$ in (1) using the observed input/output data

of sampled continuous time CNN patterns. Generally, the form of the CML model $f(\cdot)$ is unknown, so it is necessary to expand f using a known set of possible candidate model terms. Equation (1) can also be written in a regression format which is constructed as a linear combination of a finite number of model terms.

$$y_i(k) = \sum_k \theta_{i,m}\varphi_{i,m}(k) + \varepsilon_i(k) \tag{9}$$

Here, model terms $\varphi_{i,m}(k)$ are composed of $q^{n_y}y_i(k)$, $q^{n_u}u_i(k)$, $q^{n_y}s^{m_y}y_i(k)$, $q^{n_u}s^{m_u}u_i(k)$ which represent the influence of past inputs and outputs from both the local and neighboring lattices.

3 A CML Identification Algorithm for Cellular Neural Network Patterns

3.1 The selection of the sampling interval for the identification data

The selection of the sampling interval of the original continuous data in system identification could have a great influence on the term structure selection and parameter estimation of the identified model. For example, if the identification data is over-sampled, the regression matrix will become ill-posed due to the high correlation between successive measurements. On the other hand, if the data for identification is under-sampled, important dynamic information will be lost. In these situations, the final derived model is more likely to be ill-posed and sensitive to new training data or to noise.

The sampling time of the identification data from the CNN patterns which are continuously evolving over a discrete lattice needs to be appropriately determined to ensure the regression matrix is well defined. In this section, a correlation function based method [4] [6] [22] will be used to select an appropriate sampling procedure. Compared with other methods which are mostly based on information theoretical tools, the correlation method is quite simple and robust to noise. The main concept behind this method is to select proper time intervals so that the dynamic information in the patterns are retained in the identification data.

The selection procedure for the sampling time is based on the linear and nonlinear functions defined as follows.

$$\Phi_{yy}(\tau) = \frac{\sum_{(i,k)=S(0)}^{S(N_s-1)}(y_i(k)-\overline{y})(y_i(k-\tau)-\overline{y})}{\sum_{(i,k)=S(0)}^{S(N_s-1)}(y_i(k)-\overline{y})^2} \tag{10a}$$

$$\Phi_{y^2y^2}(\tau) = \frac{\sum_{(i,k)=S(0)}^{S(N_s-1)}(y_i^2(k) - \overline{y^2})(y_i^2(k-\tau) - \overline{y^2})}{\sum_{(i,k)=S(0)}^{S(N_s-1)}(y_i^2(k) - \overline{y^2})^2} \tag{10b}$$

In (10), N_s samples of the original spatiotemporal data is collected from outputs that are randomly selected over both the space and time domain, and $\overline{\cdot}$ denotes the averaging operation over the specific domain defined by the selection vector S. On the basis of the above equations, both the linear and nonlinear correlation relationships of the data can therefore be measured. The minimum time values associated with the correlation functions can be defined.

$$\tau_m = min\{\tau_y, \tau_{y^2}\} \tag{11}$$

where τ_y and τ_{y^2} are time values of the first minimum of $\phi_{yy}(\tau)$ and $\phi_{y^2y^2}(\tau)$ respectively. In practice, the 95% confidence limits which are equal to $\pm 1.96/\sqrt{N_s}$ are usually used to replace the minimum values of the above correlation functions

The sampling intervals T for the spatiotemporal data in the time domain [1] can be chosen by following the rule of thumb.

$$\frac{\tau_m}{20} \leq T \leq \frac{\tau_m}{10} \tag{12}$$

In practical applications, this simple but effective empirical method appears to work well.

3.2 The identification algorithm

The identification problem for spatiotemporal systems is composed of two parts: model term selection and parameter estimation. The Orthogonal Forward Regression (OFR) algorithm which involves a stepwise orthogonalisation of the regressors and a forward selection of the significant terms based on the Error Reduction Ratio (ERR) criterion [5] has been successfully applied to identify a wide class of spatiotemporal systems [8] [9] [12]. Using this method, the model structure is selected step by step by comparing the ERRs of all possible model terms from a set of candidate regressors $\{\varphi_m\}_{m=1}^{M}$ which are defined in (9). The term coefficients are computed afterwards according to the orthogonalisation matrix. As a typical feature of the CNN model structure, the nonlinear piecewise function in (7) plays an important role in triggering the formation of self organized spatiotemporal patterns. Apart from the importance of ensuring the stability of the CNN model, the output function also defines the range of the output variable. However, from the viewpoint of model identification, it is not easy to approximate this simple nonlinear function using available nonlinear basis functions (Radial Basis

Functions, Kernel Basis Functions, Polynomials and Wavelets) which are currently widely used in model identification.

In this section, a new identification method for autonomous CNN patterns is proposed to solve this problem. The format of the revised CML model for CNN pattern identification is defined as follows.

$$y_i(k) = g(f'(q^{n_y} y_i(k), q^{n_y} s^{m_y} y_i(k))) + \varepsilon_i(k) \tag{13}$$

The function $g(\cdot)$ is the same as defined in (7). The incorporation of the function $g(\cdot)$ ensures that the output of the identified CML model will evolve within a certain region. The main aim of identifying the CML model for CNN patterns is then to determine the unknown function $f'(\cdot)$ in (13).

The two corresponding One-Step-Ahead (OSA) prediction errors associated with function $f'(\cdot)$ in (13) can be expressed as

$$\varepsilon_i^{(osa)}(k) = \quad y_i(k) - y_i^{(osa)}(k) = \quad y_i(k) - g(f'(q^{n_y} y_i(k), q^{n_y} s^{m_y} y_i(k))) \tag{14}$$

$$\varepsilon_i'^{(osa)}(k) = \quad y_i(k) - y_i'^{(osa)}(k) = \quad y_i(k) - f'(q^{n_y} y_i(k), q^{n_y} s^{m_y} y_i(k)) \tag{15}$$

where $\varepsilon_i(k)$ is the actual OSA prediction error and $\varepsilon_i'(k)$ is the original OSA prediction error without considering the impact of the output function $g(\cdot)$.

It is well known that the OFR identification method is a least squares based algorithm and the aim of traditional CML identification algorithm is to obtain a final CML model based on the sum of the squared OSA prediction error $\sum_{i,k} \varepsilon_i^2(k)$. The ERR can be expressed as

$$ERR_m = \frac{g_m^2 w_m^T w_m}{Y^T Y}, g_m = \frac{w_m^T Y}{w_m^T w_m} \tag{16}$$

where w_m is the orthogonalised regressor associated with term φ_m and g_m is the corresponding estimated coefficient. However, when the standard OFR algorithm is applied to obtain the model $f'(\cdot)$ in (13), it can be easily seen from (16) that the influence of the nonlinear output function $g(\cdot)$ is not taken into account during the ERR computation. For example, when $y_i(k) = 1$ and $y_i'^{(osa)} = f'(q^{n_y} y_i(k), q^{n_y} s^{m_y} y_i(k)) > 1$, the actual OSA prediction error $\varepsilon_i(k)$ in (14) should be 0 but $\varepsilon_i'(k)$ will not be equal to 0 when the output function $g(\cdot)$ is not taken into account. In this situation, ERR which is used to measure the proportional contribution of each term to the variance of the overall dependent variables may provide incorrect information for term selection. Similar problems would also arise during the computation of the associated coefficients.

To solve this problem, a new identification method based on the OFR algorithm is proposed to obtain a CML model in (13) by taking into account the impact of the nonlinear output function. The model terms are

selected step by step by comparing the sum of the squared OSA prediction error $\sum_{i,k} \varepsilon_i^2(k)$ during every orthogonalisation stage. The estimates of the corresponding coefficients are then adjusted using the updated output vector according to the nonlinear function $g(\cdot)$.

In summary, the amended OFR algorithm for identifying this class of CNN patterns is outlined as below.

Step j=1: Select the first model term with the smallest prediction error

$$I_1 = I_M = \{1, 2, ..., M\}, Y_1 = Y \tag{17}$$

$$w_i(k) = \varphi_i(k), \hat{b}_i = \frac{[w_i, Y_i]}{[w_i, w_i]} \tag{18}$$

Find the term with the smallest prediction error.

$$l_1 = arg \min_{i \in I_1} \left(Y_1^T Y_1 - \hat{b}_i^2 w_i^T w_i \right) \tag{19}$$

Compute the coefficient of the selected term.

$$p_1 = w_{l_1}, c_1 = \frac{[p_1, Y_1]}{[p_1, p_1]}, a_{1,1} = 1 \tag{20}$$

Update the output vector Y_2 according to the first model prediction.

$$y_1^{(osa)}(k) = c_1 * p_1(k)$$

If $|y_1^{(osa)}(k)| > 1$,then

$$y_2(k) = y_1^{(osa)}(k),$$

else

$$y_2(k) = y_1(k), k = 1, 2, \ldots, N$$

Stepj,$j = 2, 3, ...$: Iteratively orthogonalise the remaining regressors one by one to select the next model term with the smallest prediction error among the remaining candidate terms.

$$I_j = I_{j-1} \setminus l_j - 1 \tag{21}$$

Orthogonalise the model regressors.

$$w_i(k) = \varphi_i(k) - \sum_{m=1}^{j-1} \frac{[p_m, Y_j] p_m}{[p_m, p_m]}, \hat{b}_i = \frac{[w_i, Y_j]}{[w_i, w_i]} \tag{22}$$

Find the model term with the smallest prediction error.

$$l_j = arg \min_{i \in I_j} \left(Y_j^T Y_j - \sum_{m=1}^{j-1} c_m^2 p_m^T p_m - w_i^T w_i \right) \tag{23}$$

Compute the coefficient of the selected term.

$$p_j = w_{l_j}, c_j = \frac{[p_j, Y_j]}{[p_j, p_j]}, a_{m,j} = \frac{[p_m, \varphi_{l_j}]}{[p_m, p_m]}, m = 1, 2, ..., j-1 \tag{24}$$

Update the output vector Y_{j+1} according to the model prediction at stage j.

$$y_j^{(osa)}(k) = \sum_{m=1}^{j} c_m * p_m(k)$$

If $|y_j^{(osa)}(k)| > 1$, then

$$y_{j+1}(k) = y_j^{(osa)}(k),$$

else if $y_j(k) > 1$,

$$y_{j+1}(k) = 1$$

else

$$y_{j+1}(k) = y_j(k), k = 1, 2, \ldots, N$$

This procedure is terminated at the M_s-th step when a required number of terms has been selected in the final model. The estimated coefficients $\Theta = \{\theta_m\}_{m=1}^{m=M_s}$ associated with the selected terms$\{\varphi_{l_m}\}_{m=1}^{m=M_s}$ are computed using

$$\Theta = \mathbf{A}^{-1}C, \tag{25}$$

where $\mathbf{A} = \{a_{m,j}\}$ is an upper-triangular matrix which is defined above and $C = (c_1, c_2, ..., c_{M_s})$ is the coefficient vector associated with the orthogonalised terms $\{p_m\}_{m=1}^{M_s}$.
In this new model identification algorithm, the summation of squared one-step-ahead prediction errors associated with every term selection is employed as a criterion for model term selection. The values of the one-step-ahead prediction error and term coefficients at each step are adjusted by updating the output vector when the output prediction falls within the saturation region associated with the definitions of the CNN models. Using this approach, the prediction performance of the identified model can be greatly improved.

4 Numerical Examples

In this section, three different kinds of spatiotemporal patterns, *Checkerboards*, *Stripes* and *Squiggles*, which are generated by autonomous CNN models with zero-threshold are investigated. The input/output data for identification was randomly sampled from the initial random state to the final

stable equilibrium state. The proposed CML model (13) and the identification algorithm described above were then applied. In these examples, the model predicted output was simulated to test the prediction performance and dynamical characteristics of the new identified CML model. The model predicted output $y_{i,j}^{(mpo)}(k)$ is defined as follows,

$$y_{i,j}^{(mpo)}(k) = g(f'(q^{n_y} y_{i,j}^{(mpo)}(k), q^{n_y} s^{m_y} y_{i,j}^{(mpo)}(k))) \tag{26}$$

where $g(\cdot)$ is the output function defined in (7) and $f'(\cdot)$ is the new identified CML model.

4.1 Example 1: Checkerboard Patterns

In the first example, the checkerboard like patterns which evolve over a two dimensional space are considered. The A-template of the CNN model (13) to generate the checkerboard patterns was set as

$$A = \begin{pmatrix} 0.125 & -0.25 & 0.125 \\ -0.25 & 0 & -0.25 \\ 0.125 & -0.25 & 0.125 \end{pmatrix} \tag{27}$$

where the radius of the coupling neighborhood was 1. The initial simulation state $x_{i,j}(0)$ for the checkerboard patterns was randomly distributed between -0.1 and 0.1. The zero-flux conditions where the state-variable is reflected across the boundary was chosen as the boundary conditions. The CNN model with the above settings was then numerically simulated with a time step $\Delta k = 0.1$ over the space domain 100×100. To determine the appropriate sampling time for the identification data, the correlation tests which were proposed in Section 3.1 were computed. From the results given in Figure (1), it can be seen that the sampling time T should be chosen between $\tau_m/10 = 64/10 = 6.4$ and $\tau_m/20 = 64/20 = 3.2$. Following the empirical selection procedure, the sampling time in this example was chosen to be 5. The patterns of the system output at different times are plotted in Figure (2).

The new identification procedure proposed in Section 3.2 was performed with $N = 3600$ data randomly sampled from the space and time domain. The traditional CML identification algorithm [8] [9] was applied to provide a comparison with the new methods introduced above. The identified model terms and the corresponding coefficients are given in Table(1), where the terms $y_{1,i,j}(k-1)$ and $y_{2,i,j}(k-1)$ represent the combined output variables of the neighbouring sites around the lattice (i, j), which are defined below to ensure a symmetric topology of coupling variables.

$$y_{1,i,j}(k) = y_{i-1,j}(k) + y_{i+1,j}(k) + y_{i,j-1}(k) + y_{i,j+1}(k) \tag{28}$$

$$y_{2,i,j}(k) = y_{i+1,j-1}(k) + y_{i+1,j+1}(k) + y_{i-1,j-1}(k) + y_{i-1,j+1}(k) \tag{29}$$

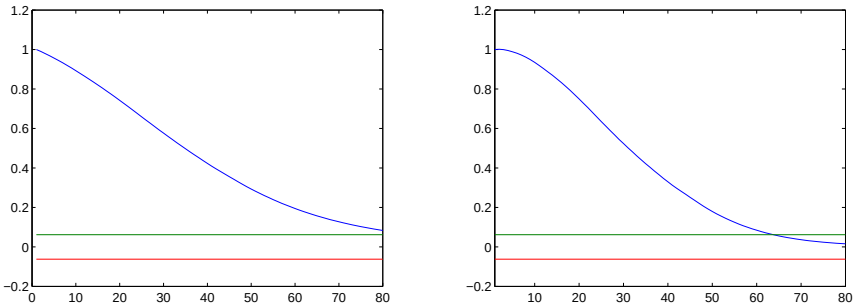

Figure 1: Correlation functions $\phi_{yy}(\tau)$ (left) and $\phi_{y^2y^2}(\tau)$ (right) from (10) calculated from $N_s = 1000$ random data samples of the checkerboard patterns in Example 1. It can be seen that the minimum time value is $\tau_m = \tau_{y^2} \approx 64$.

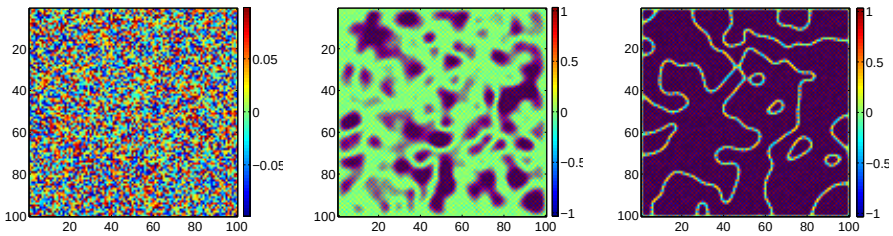

Figure 2: Snap shots of the CNN system simulation output for the checkerboard patterns at the times $k = 1, 20, 40$ for Example 1, .

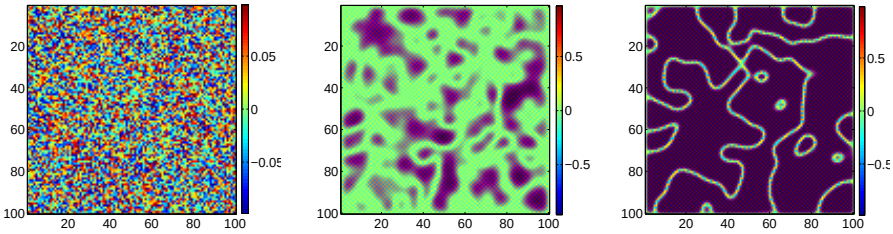

Figure 3: Snap shots of the model predicted output of the identified model using the new algorithm at the times $k = 1, 20, 40$ for Example 1.

The model predicted outputs (26) were simulated using the identification results in Table (1). Some snap shots of the model predicted outputs of the two identified models are shown in Figure (3),(4). It can be seen from Figure

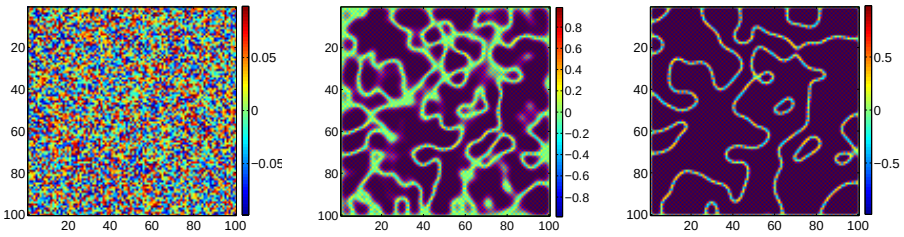

Figure 4: Snap shots of the model predicted output of the identified model using the standard algorithm at the times $k = 1, 20, 40$ for Example 1.

(3) that using the new identification algorithm, the dynamics of the original CNN patterns are well approximated by the identified CML model at every time step. However, as can be seen from the simulation results of the model identified using the standard CML method, the model predicted output at time $t = 20$ is quite different from the system output at that time.

4.2 Example 2: Stripe Patterns

Consider the CNN model with the A-template for the stripe patterns.

$$A = \begin{pmatrix} -0.2 & 0 & -0.2 \\ 0 & 0.8 & 0 \\ -0.2 & 0 & -0.2 \end{pmatrix} \tag{30}$$

The initial state $x_{i,j}(0)$ for the stripe patterns was randomly distributed between -0.1 and 0.1. Zero-flux boundary conditions were chosen. The above CNN model was numerically simulated with a time step $\Delta k = 0.1$ over the space domain 100×100.

The correlation based tests of the original data were applied to determine an appropriate sampling interval for the identification data. According to the simulation results in Figure (5) and the empirical selection method, the sampling time T can be chosen between $\tau_m/10 = 44/10 = 4.4$ and $\tau_m/20 = 44/20 = 2.2$. Here, the sample time for the identification data was chosen to be 3. Figure (6) shows snap shots of the system output at different times.

Both the proposed identification method and the standard OFR based CML identification algorithm were applied to obtain CML models for the stripe patterns in this example. Table (2) gives the identified results obtained from the two different algorithms. The terms $y^{(1)}_{i,j}(k-1)$ and $y^{(2)}_{i,j}(k-1)$ denote the same combined variables of the neighbouring outputs as defined in the first example (28).

Table 1: Terms and parameters of the identified CML models for the checkerboard pattern in Example 1

Term order	Model terms	Estimated parameters using the new algorithm
1	$y_{i,j}(k-1)$	0.4660
2	$y_{1,i,j}(k-1)$	-0.1348
3	$y^2_{2,i,j}(k-1)$	0.0017
4	$y^2_{1,i,j}(k-1)$	-0.0023
5	$y^2_{i,j}(k-1)$	0.0108
6	$y_{2,i,j}(k-1)$	0.0752
7	$y^3_{i,j}(k-1)$	0.0384
8	$y^3_{1,i,j}(k-1)$	0.0033
9	$y^3_{2,i,j}(k-1)$	-0.0019
Term order	Model terms	Estimated parameters using the standard algorithm
1	$y_{i,j}(k-1)$	0.3814
2	$y^3_{i,j}(k-1)$	0.0154
3	$y_{1,i,j}(k-1)$	-0.1479
4	$y^3_{1,i,j}(k-1)$	0.0025
5	$y_{2,i,j}(k-1)$	0.1009
6	$y^3_{2,i,j}(k-1)$	-0.0036
7	$y^2_{i,j}(k-1)$	0.0024
8	$y^2_{2,i,j}(k-1)$	0.0008
9	$y^2_{1,i,j}(k-1)$	-0.0010

To test the prediction performance, model predicted outputs as defined in (26) were simulated using the different identification results given in Table (2). Some snap shots of the model predicted outputs of two identified models are shown in Figure (7), (8). It can be seen from Figure (7) that the final CML model identified using the new algorithm shows better prediction capabilities than the second identified CML model and the pattern formation of stripes is repeated by the identified model over a long term simulation.

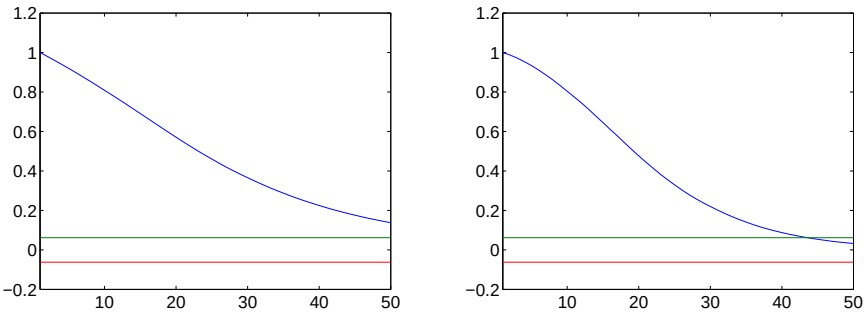

Figure 5: Correlation functions $\phi_{yy}(\tau)$ (left) and $\phi_{y^2y^2}(\tau)$ (right) from (10) calculated from $N_s = 1000$ random data samples of the stripe patterns in Example 2. It can be seen that the minimum time value is $\tau_m = \tau_{y^2} \approx 44$.

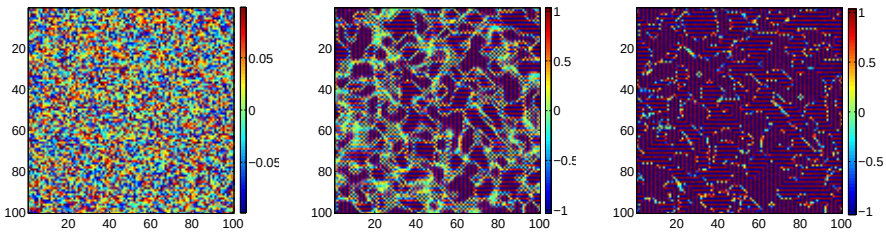

Figure 6: Snap shots of the CNN system simulated output for the stripe patterns at the times $k = 1, 30, 60$ for Example 2.

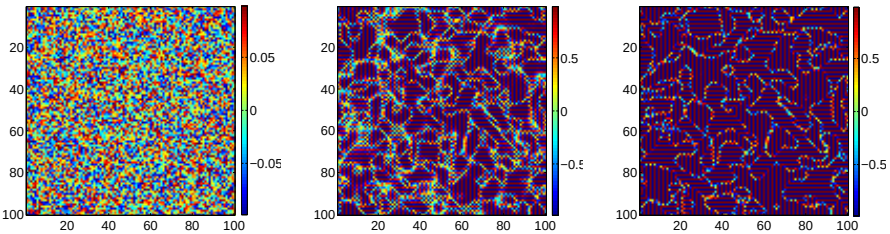

Figure 7: Snap shots of the model predicted output of the identified model using the new algorithm at the times $k = 1, 30, 60$ for Example 2.

4.3 Example 3: Squiggle Patterns

The squiggle like patterns are considered in this example. The CNN patterns are generated with the following A-template of CNN model in a two

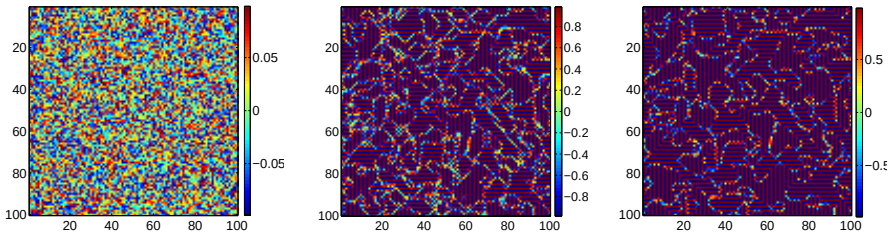

Figure 8: Snap shots of the model predicted output of the identified model using the standard algorithm at the times $k = 1, 30, 60$ for Example 2.

dimensional space.

$$A = \begin{pmatrix} -0.25 & -1.0 & -1.5 & -1.0 & -0.25 \\ -1.0 & 2.5 & 7.0 & 2.5 & -1.0 \\ -1.5 & 7.0 & -23.25 & 7.0 & -1.5 \\ -1.0 & 2.5 & 7.0 & 2.5 & -1.0 \\ -0.25 & -1.0 & -1.5 & -1.0 & -0.25 \end{pmatrix} \tag{31}$$

In this example, the radius of the coupling neighborhood was set to be 2. The random initial state $x_{i,j}(0)$ for the squiggle patterns was uniformly distributed between -0.1 and 0.1. Zero-flux boundary conditions were chosen. The CNN model with the above settings was numerically simulated with a time step $\Delta k = 0.1$ over the space domain 60×60.

Initially, the correlation based tests were applied to determine a sampling interval for the identification data. According to the simulation results in Figure (9), the sampling time T can be chosen between $\tau_m/10 = 160/10 = 16$ and $\tau_m/20 = 160/20 = 8$. In this example, the sample time for the identification data was chosen to be 10. Figure (10) shows some snap shots of the system output of the squiggle patterns at different times.

Two CML models were identified using both the new proposed algorithm and the standard algorithm. Table (3) gives the identified results from the two algorithms. The terms $y_{1,i,j}(k-1)$ and $y_{2,i,j}(k-1)$ denote the same combined variables as defined in the first example (28). Other terms in Table (3) are defined as follows

$$\begin{aligned} y_{3,i,j}(k) &= y_{i,j-2}(k) + y_{i,j+2}(k) + y_{i-2,j}(k) + y_{i+2,j}(k) \\ y_{4,i,j}(k) &= y_{i-1,j-2}(k) + y_{i-1,j+2}(k) + y_{i+1,j-2}(k) + \\ &\quad y_{i+1,j+2}(k) + y_{i-2,j-1}(k) + y_{i-2,j+1}(k) + y_{i+2,j-1}(k) + y_{i+2,j+1}(k) \\ y_{5,i,j}(k) &= y_{i-2,j-2}(k) + y_{i-2,j+2}(k) + y_{i+2,j-2}(k) + y_{i+2,j+2}(k) \end{aligned}$$

Table 2: Terms and parameters of the identified CML models for the stripe pattern formation in Example 2

Term order	Model terms	Estimated parameters using the new algorithm
1	$y_{i,j}(k-1)$	0.9239
2	$y^3_{1,i,j}(k-1)$	-0.0015
3	$y^2_{1,i,j}(k-1)$	-0.0018
4	$y_{1,i,j}(k-1)$	0.0039
5	$y^2_{2,i,j}(k-1)$	0.0001
6	$y^2_{i,j}(k-1)$	-0.0010
7	$y_{2,i,j}(k-1)$	-0.0711
8	$y^3_{1,i,j}(k-1)$	-0.0529
9	$y^3_{2,i,j}(k-1)$	0.0024
Term order	Model terms	Estimated parameters using the standard algorithm
1	$y_{i,j}(k-1)$	0.9729
2	$y^3_{i,j}(k-1)$	-0.1123
3	$y_{2,i,j}(k-1)$	-0.0711
4	$y^3_{2,i,j}(k-1)$	0.0023
5	$y^2_{i,j}(k-1)$	-0.0030
6	$y^3_{1,i,j}(k-1)$	-0.0044
7	$y^2_{2,i,j}(k-1)$	0.0002
8	$y_{1,i,j}(k-1)$	0.0023
9	$y^2_{1,i,j}(k-1)$	-0.0014

Some snap shots of the model predicted outputs of two identified models in Table (3) are shown in Figure (11),(12). According to comparisons between Figure (11) and Figure (12), it can be seen that the CML models which were identified using the two different algorithms produce good approximations of the squiggle patterns. Both two identification algorithms show similar performance for the squiggle patterns.

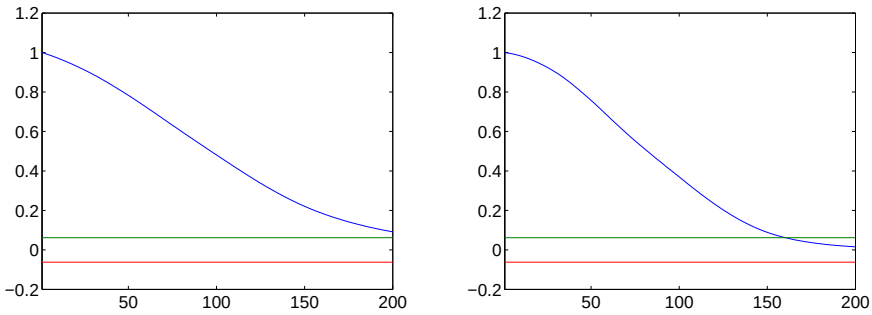

Figure 9: Correlation functions $\phi_{yy}(\tau)$ (left) and $\phi_{y^2y^2}(\tau)$ (right) form (10) calculated from $N_s = 1000$ random data samples of the squiggle patterns in Example 3. It can be seen that the minimum time value is $\tau_m = \tau_{y^2} \approx 44$.

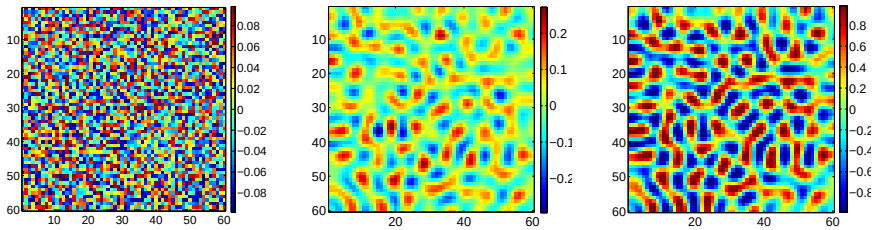

Figure 10: Snap shots of the CNN system simulation output of the squiggle patterns at the times $k = 1, 12, 24$ for Example 3.

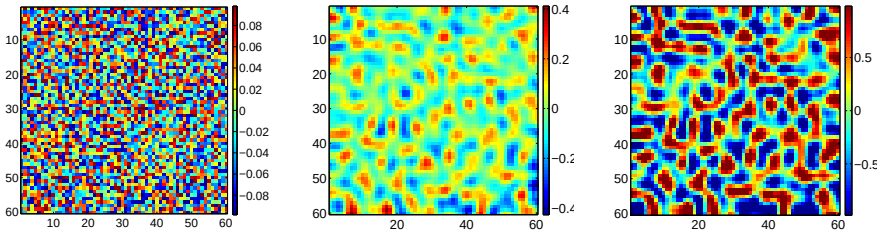

Figure 11: Snap shots of the model predicted output of the identified model using the new algorithm at the times $k = 1, 12, 24$ for Example 3.

5 Conclusions

The identification of models to represent the patterns formed from CNN simulations has been investigated in this paper. The CNN patterns represent

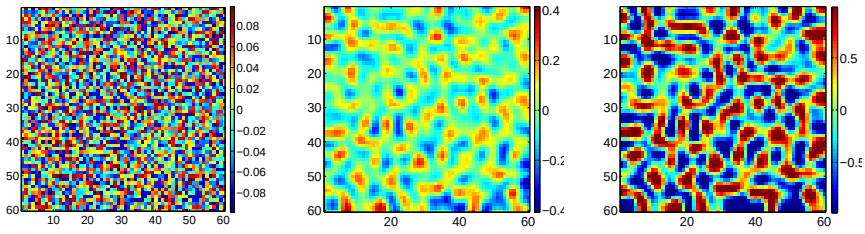

Figure 12: Snap shots of the model predicted output of the identified model using the standard algorithm at the times $k = 1, 12, 24$ for Example 3.

Table 3: Terms and parameters of the identified CML models for the squiggle pattern formation in Example 3

Term order	Model terms	Estimated parameters using the new algorithm
1	$y_{1,i,j}(k-1)$	0.2074
2	$y_{i,j}(k-1)$	0.3034
3	$y_{5,i,j}(k-1)$	-0.0484
4	$y_{3,i,j}(k-1)$	-0.0809
5	$y_{2,i,j}(k-1)$	0.1265
6	$y_{4,i,j}(k-1)$	-0.0062
Term order	Model terms	Estimated parameters using the standard algorithm
1	$y_{i,j}(k-1)$	0.7508
2	$y_{1,i,j}(k-1)$	0.1065
3	$y_{3,i,j}(k-1)$	-0.0264
4	$y_{5,i,j}(k-1)$	-0.0044
5	$y_{2,i,j}(k-1)$	-0.0067
6	$y_{4,i,j}(k-1)$	-0.0007

a subset of spatiotemporal systems which produce interesting phenomena in many areas. A special type of CML model with output constraints and a new identification algorithm has been proposed to yield models with good prediction performance. The main difference of the proposed algorithm is the adjustment of the term coefficients based on a modified prediction error sequence during the orthogonalisation process. The numerical examples demonstrate that the identified model can well predict and reproduce the

dynamics of the CNN patterns over the long term.

6 Acknowledgements

The authors gratefully acknowledge that this work was supported by EPSRC(UK).

References

[1] H. D. I. Abarbanel, R. Brown, and J. B. Kadtke, *Prediction in chaotic nonlinear systems: Methods for time series with broadband fourier spectra*, Phys. Rev. A **41** (1990), 1782–1807.

[2] P. Arena, S. Baglio, L. Fortuna, and G. Manganaro, *Self-organization in a two-layer cnn*, IEEE Trans. Circuits Sys. I **42** (1998), 157–162.

[3] R. A. Barrio, C. Varea, J. L. Aragon, and P. K. Maini, *A two-dimensional numerical study of spatial pattern formation in interacting turing systems*, Bull. Math. Bio. **61** (1999), 483–505.

[4] S. A. Billings and L. A. Aguirre, *Effects of the sampling time of the dynamics and identification of nonlinear models*, Int. J. Bifurcation and Chaos **5** (1995), 1541–1556.

[5] S. A. Billings, S. Chen, and M. J. Kronenberg, *Identification of mimo non-linear systems using a forward regression orthogonal estimator*, Int. J. Control **49** (1988), 2157–2189.

[6] S. A. Billings and Q. H. Tao, *Model validity tests for non-linear signal processing applications*, Int. J. Control **54** (1991), 157–194.

[7] L. O. Chua, *Cnn: A paradigm for complexity*, World Scientific Series on Nonlinear science E, 1998.

[8] D. Coca and S. A. Billings, *Identification of coupled map lattice models of complex spatiotemporal patterns*, Phys. Lett. A **287** (2001), 65–73.

[9] ———, *Identification of finite dimensional models of infinite dimensional dynamical systems*, Automatica **38** (2003), 1851–1856.

[10] I. R. Epstein and K. Showalter, *Nonlinear chemical dynamics: oscillations, patterns, and chaos*, J. Phys. Chem. **100** (1996), 13132–13147.

[11] P. Gray and S. K. Scott, *Autocatalytic reactions in the isothermal, continuous stirred tank reactor - isolas and other forms of multistability*, Chem. Eng. Sci **38** (1983), 29–43.

[12] L. Z. Guo and S. A. Billings, *Identification of coupled map lattice models of stochastic spatio-temporal dynamics using wavelets*, Dynamical System **19** (2004), 265–278.

[13] M. Itoh and L. O. Chua, *Image processing and self-organizing cnn*, Inter. J. Bifurcation and Chaos **15** (2005), 2939–2958.

[14] K. Kaneko, *Spatiotemporal intermittency in coupled map lattices*, Prog. Theor. Phys. **74** (1985), 1033–1044.

[15] ———, *Turbulence in coupled map lattices*, Physica D **18** (1986), 475–476.

[16] ———, *Pattern dynamics in spatiotemporal chaos pattern selection, diffusion of defect and pattern competition intermittency*, Physica D **34** (1989), 1–41.

[17] K. J. Lee, W. D. McCormick, Q. Ouyang, and H. L. Swinney, *Pattern formation by interacting chemical fronts*, Science **16** (1993), 192–194.

[18] J. L. Maron and S. Harrison, *Spatial pattern formation in an insect host-parasitoid system*, Science **278** (1997), 1619–1621.

[19] H. Meinhardt, *The algorithm beauty of sea shells*, Springer-Verlag, 1995.

[20] J. D. Murray, *Mathematical biology*, Springer-Verlag, 1989.

[21] Q. Ouyang and H. L. Swinney, *Transition from a uniform state to hexagonal and striped turing patterns*, Nature **352** (1991), 610–612.

[22] Y. Pan and S. A. Billings, *The identification of complex spatiotemporal patterns using coupled map lattice models*, Submitted for publication.

[23] B. E Shi and T. Luo, *Spatial pattern formation via reaction-diffusion dynamics in 32x32x4 cnn chip*, IEEE Trans. Circuits Sys. I **51** (2004), 939–947.